Title page

Title

2 new cases of pontocerebellar hypoplasia type 10 identified by whole exome sequencing in a Turkish family

Authors

Mohamed Wafik[a]
John Taylor[b]
Tracy Lester[b]
Richard J. Gibbons[c]
Deborah J Shears [a]

Affiliation

[a] Oxford Centre for Genomic Medicine, Oxford University Hospitals NHS Foundation Trust, Oxford, UK
[b] Oxford Medical Genetics Laboratories, Oxford University Hospitals NHS Foundation Trust, Oxford, UK
[c] MRC Molecular Haematology Unit, Weatherall Institute of Molecular Medicine, University of Oxford, Oxford, UK

Running title: pontocerebellar hypoplasia type 10

Conflict of interest disclosures: None

Corresponding author

Mohamed Wafik

Email: mohamed.wafik@ouh.nhs.uk

Telephone: +44 (0) 1865227207

Address:

OxGEM: Oxford Centre for Genomic Medicine
ACE building, Nuffield Orthopaedic Centre
Oxford University Hospitals NHS Foundation Trust
Windmill Road
Headington
Oxford, OX3 7HE

Abstract

Pontocerebellar hypoplasia type 10 (PCH10) is a progressive autosomal recessive neurodegenerative disorder that has been recently described in association with *cleavage and polyadenylation factor I subunit 1* (*CLP1*) mutations. To date, all reported cases have the same homozygous missense mutation in the *CLP1* gene suggesting a founder mutation. CLP1 is an RNA kinase involved in tRNA splicing and maturation. There is evidence that the mutation is associated with functionally impaired kinase activity and subsequent defective tRNA processing. Through whole exome sequencing, we identified the same mutation in an extended family of Turkish origin. Both children presented with severe psychomotor delay, progressive microcephaly, and constipation. However, intrafamilial phenotypic variability is suggested due to the variability in their brain abnormalities and clinical features.

Keywords

Pontocerebellar hypoplasia type 10; autosomal recessive; founder mutation; whole exome Sequencing; CLP1

Main Text:

Introduction:

Pontocerebellar hypoplasia type 10 (PCH10)(OMIM# 615803) is a rare genetic disorder that has been recently described, simultaneously and independently, by Karaca *et al.,* and Schaffer *et al.,* in 2014. It is characterized by severe psychomotor delay, progressive microcephaly, spasticity, epileptic seizures and structural brain abnormalities. Additional features include axonal sensorimotor neuropathy and craniofacial dysmorphism. The condition exhibits an autosomal recessive mode of inheritance and belongs to the progressive neurodegenerative pontocerebellar hypoplasia group of disorders (Schaffer *et al.,* 2014).

To date, few cases of PCH10 have been described in the literature. Interestingly, all reported cases have the same homozygous missense mutation in the *CLP1* gene, NM_006831.2:c.419G>A; p.(Arg140His), and come from consanguineous families in the eastern part of Turkey (Karaca *et al.,* 2014, and Schaffer *et al.,* 2014).

CLP1 is an RNA kinase that was first discovered by Weitzer and Martinez in 2007. It is involved in tRNA biogenesis and maturation. tRNAs play an important role in protein biosynthesis by carrying the amino acids to the ribosome for translation. Like other RNA molecules, tRNAs undergo post-transcriptional modifications, for example splicing, to transform the pre-tRNA form to the fully functioning mature form (Hanada *et al.,* 2013). Notably, few tRNAs undergo splicing in humans as only 6% of human tRNA genes contain introns (Paushkin *et al.*, 2004).CLP1 interacts with the tRNA splicing endonuclease (TSEN) complex which is essential in pre-tRNA splicing and maturation (Hanada *et al.,* 2013). *CLP1* loss of function has been shown to affect TSEN stabilization and tRNA splicing, and deplete mature tRNA, leading to defective tRNA processing and maturation. Even though tRNA maturation is vital in all cells, a defect in their processing has been strongly associated with neurological disorders (Karaca *et al.,* 2014).

Here, we report on two children from the same extended family of Turkish origin. Both presented with severe global developmental delay, progressive microcephaly, and structural brain abnormalities with an overlapping phenotype. Although the families were not aware of any consanguinity, both children (Fig.1) were found to have the same recessive founder mutation previously described in PCH10 (Karaca *et al.,* 2014), suggesting that their parents are distantly related.

Clinical report:

The proband, a female (III.6, Fig.1) aged 4 years, is the first child born to healthy parents of Turkish origin. The paternal age was 38 years and the maternal age was 34 years when the child was born. The family history was remarkable in that the proband's first cousin once removed (IV.1, Fig.1) had significant developmental delay and microcephaly of unknown cause.

Patient 1

III.6 was conceived by invitro fertilization. The pregnancy was uncomplicated and she was born at 41 weeks by vacuum-assisted vaginal delivery. At birth, her weight was 3.5 Kg and her head circumference was 34 cm (z-score: 0.10). Apart from some jitteriness in the neonatal period, her perinatal history was unremarkable.

At 12 months, she presented with significant gross and fine motor skills delay, constipation and feeding difficulties, truncal hypotonia, head lag, and increased muscles tone in all limbs. Her weight was 8.74 kg, her head circumference was 41 cm (z-score: −3.79), and her height was 81.3 cm (z-score: 0.20) at 18 months. At 2 years, she had three capillary vascular malformations. Her ophthalmological evaluation revealed alternating exotropia with slightly limited adduction in both eyes, and horizontal saccadic innervation weakness. She had subtle dysmorphic features in the form of high arched eyebrows, a slightly low hanging columella, tapered fingers, and kyphoscoliosis (Fig.2A, 2B, Table 1). In view of the microcephaly and the capillary malformations, microcephaly-capillary malformation syndrome was excluded in her (Table 2). At 3 years, an episode of possible seizures was noted and, although the EEG did not capture frank seizure activity, the findings were suggestive of a potential for multifocal seizures. At that time, she had severe global developmental delay and could only say two words in Turkish language.

Patient 2

Subsequently, her relative (**IV.1**, Fig.3), who is the first child born to healthy Turkish parents, was reviewed. At birth, the paternal age was 37 years and the maternal age was 28. She presented with severe global developmental delay, progressive microcephaly, constipation, and visual impairment. Her visual problems included strabismus, nystagmus, hypermetropia, astigmatism, visual impairment, and cone-rod dystrophy. She had bilateral hip subluxation and underwent bilateral proximal femoral osteotomies and bilateral Dega procedures. At 5 years, she could not say single words. She was noted to have more significantly prominent dysmorphic features than III.6 including bi-temporal narrowing, marked synophrys, long palpebral fissures, divergent squint, a broad nasal root, low hanging columella, widely spaced teeth, a short neck, tapered fingers, and hypertrichosis of her upper and lower limbs.

Both patients had evident structural brain abnormalities reported on MRI brain scans (summarized in Table 3). The dysmorphic and clinical features of both children are summarized in Tables 1 and 4 respectively.

Clinical summary:

Generally, III.6 and IV.1 presented with similar clinical manifestations. However, it was clearly evident that IV.1 had more severe visual abnormalities, developmental delay (Table 4), and craniofacial dysmorphism (Table 1) than III.6. Nevertheless, III.6 had epileptic seizures which were not described in IV.1 (Table 4).

Results:

Trio-based exome sequencing was performed for III.6 and her parents at The Wellcome Trust Sanger Institute, using their standard protocol. SureSelect Target Enrichment System (Agilent Technologies) was used, followed by 2×100 nt paired-end sequencing on an Illumina HiSeq 2000. Raw sequence reads were aligned to the reference human genome (GRCh37).

The result showed a homozygous missense sequence variant in *CLP1*: (NM_006831.2:c.419G>A) resulting in an amino acid substitution of p.(Arg140His), both of which are positively charged polar amino acids. The variant was validated by targeted bi-directional Sanger sequencing in our laboratory and parental analysis confirmed true homozygosity.

Investigation into the pathogenicity of the variant showed that it has been previously reported in several consanguineous Turkish families in association with a phenotype of pontocerebellar hypoplasia, with segregation consistent with autosomal recessive inheritance (Karaca *et al.*, and Schaffer *et al.*, 2014). It was seen in one individual (0.03%), in a heterozygous state, in a population-based cohort of 33233 non-Finnish Europeans (Exome Aggregation Consortium). The Genome Aggregation Database (gnomAD) showed the presence of the allele in 2 individuals (1 Latino and 1 European non-Finnish), again in a heterozygous state. Review of the literature and publicly available databases did not provide an insight with regards to the mutant allele frequency in the Turkish population. Homozygosity was not seen in in-house or public databases.

The variant was predicted to be pathogenic. Subsequent screening for the mutation in IV.1, via Sanger sequencing, revealed its presence in a homozygous state, with confirmed bi-parental inheritance.

Written informed consents for publication of clinical features and photographs were obtained from parents of both families.

Discussion:

We have presented two new cases of PCH10 from the same extended family of Turkish origin. Whole exome sequencing identified the *CLP1* NM_006831.2:c.419G>A; p.(Arg140His) founder mutation in both cases. In 2014, Karaca *et al.,* and Schaffer *et al.,* described the progressive neurodegenerative disorder PCH10, with all reported cases having the same homozygous non-synonymous mutation in *CLP1*.

Brain abnormalities in PCH10:

The brain abnormalities reported in PCH10 appear to be distinct from the abnormalities associated with other types of PCH (Schaffer *et al.,* 2014). The major structural defects are cerebellar, brain stem, cortical volume loss with simplified gyral pattern, and thinning of the corpus callosum. Karaca *et al.,* 2014 suggested cortical involvement predominance in PCH10, particularly the frontal lobes. In contrast, Schaffer *et al.,* 2014 concluded that there is no difference between the abnormalities of the forebrain and the hindbrain. Pontocerebellar hypoplasia and thinning of the corpus callosum were reported in 5 patients by Schaffer *et al.*, 2014. The 6th patient had cerebellar hypoplasia and callosal body thinning with normal pontine appearance.

Although the brain imaging findings presented in our 2 cases are similar to each other and to the previously reported findings in PCH10, both patients did not show evidence of pontocerebellar hypoplasia (IV.1 showed only mild pontine hypoplasia) (Table 3, Fig.4(C), 5(C)).

While both had global reduction in white matter volume, III.6 had posterior cerebral predominance (Fig. 4(A)). Both had a reduction in the bulk of the corpus callosum as a consequence of the generalized volume loss of the white matter, as opposed to hypoplasia or developmental abnormality of the corpus callosum itself (Fig. 4(B), 5(B)).

Clinically, both patients had constipation, feeding difficulties, and skeletal manifestations (Table 4). In addition, III.6 had 3 capillary vascular malformations. None of these findings, to our knowledge, has been previously reported in PCH10.

The clinical and imaging findings presented here might imply intrafamilial phenotypic variability in PCH10, thus broadening the previously described phenotype. However, the contribution of additional environmental and genetic factors, for example additional recessive variants, especially in inbred populations, should not be overlooked. Of note, the proband's (III.6) diagnosis was established via exome sequencing which did not reveal any additional pathogenic or likely pathogenic variants. Conversely, IV.1 had a targeted genetic analysis approach, and therefore, the possibility of the presence of other likely contributing genetic variants in her has not been fully excluded.

Haplotype analysis using whole genome SNP microarray detected an extensive stretch of homozygosity (11.5Mb) in the *CLP1* region (chromosome 11) in PCH10 patients. Therefore, a founder mutation from a distant common ancestor was hypothesized (Karaca *et al.,* 2014). The findings in the extended family presented here support this hypothesis. The mutant allele was present in the 3 different branches of the family (i.e. the paternal branch of IV.1, the maternal branch of III.6, and the shared family of IV.1's maternal branch and III.6's paternal branch). This might suggest a high allele frequency in this population. Schaffer *et al.*, 2014 suggested a 1:1000 carrier frequency of the mutant allele

based on their in-house exome database which included approximately 1000 Turkish individuals. Our database search, literature review, and personal communication with Professor Dr. Beyhan Tuysuz (Department of Pediatric Genetics, Cerrahpaşa Medical School, Istanbul University, Turkey) did not provide additional information regarding the allele frequency. Undeniably, data sets provided by exome/genome databases from larger cohorts of the Turkish population would be useful in establishing a more accurate estimate of the allele frequency.

Acknowledgments

The authors are indebted to Dr Gerardine Quaghebeur and Dr Helen Stewart for their contributions to this study, and to the family for their kind participation.

Figure Titles and Legends

Fig.1 Pedigree showing the proband (III.6) and the proband's first cousin once removed (IV.1). Filled symbols represent affected individuals and open symbols represent unaffected individuals.

Fig.2 Clinical photographs of III.6, aged 2 years (A), and 4 years (B), demonstrating subtle dysmorphic features in the form of high arched eyebrows, broad nasal root, and a slightly low hanging columella.

Fig.3 Clinical photograph of IV.1 aged 5 years demonstrating more significant dysmorphic features in the form of marked synophrys, long palpebral fissures, divergent squint, broad nasal root, low hanging columella, widely spaced teeth, and a short neck.

Fig.4 MRI brain scan of III.6 at 2 years. The axial transverse weighted image (A) shows thinning of the posterior aspect of both cerebral hemispheres, as indicated by the white arrowheads. The sagittal weighted image (B) shows a reduction in the bulk of the corpus callosum as indicated by the red arrowheads. The coronal image (C) does not show evidence of cerebellar abnormalities.

Fig.5 MRI brain scan of IV.1 at 3 years. The axial transverse weighted image (A) shows global reduction in white matter volume, as indicated by the white arrowheads, with a compensatory increase in extra-axial CSF space depth. The sagittal weighted image (B) shows mild loss of bulk within the pons and the midbrain as indicated by the double white arrowheads. There is a reduction in the bulk of the corpus callosum (indicated by the red arrowheads) as a consequence of generalized white matter volume loss. The coronal image (C) does not show evidence of cerebellar abnormalities.

Table Titles and Legends

Table 1. Summary of the dysmorphic features observed in III.6 and IV.1.

Table 2. List of metabolic and genetic investigations performed for III.6 and IV.1 prior to whole exome sequencing. N/A: not available.

Table 3. List of MRI brain scan findings in III.6 and IV.1 compared to the previously reported 8 cases by Schaffer *et al.*, 2014. N/A: not available.

Table 4. List of clinical features in III.6 and IV.1 compared to the previously reported 8 cases by Schaffer *et al.*, 2014. N/A: not available. NA: not available.

References

Exome Aggregation Consortium (ExAC), Cambridge, MA (URL: <<http://exac.broadinstitute.org>>) [December, 2016]

Hanada T, Weitzer S, Mair B, Bernreuther C, Wainger BJ, Ichida J, Hanada R, Orthofer M, Cronin SJ, Komnenovic V, et al (2013). CLP1 links tRNA metabolism to progressive motor-neuron loss. *Nature* **495**:474-480.

Karaca E, Weitzer S, Pehlivan D, Shiraishi H, Gogakos T, Hanada T, Jhangiani SN, Wiszniewski W, Withers M, Campbell IM , et al (2014). Human CLP1 mutations alter tRNA biogenesis, affecting both peripheral and central nervous system function. *Cell* **157(3):**636-650.

Paushkin SV, Patel M, Furia BS, Peltz SW, Trotta CR (2004). Identification of a human endonuclease complex reveals a link between tRNA splicing and pre-mRNA 3′ end formation. *Cell* **117:**311–321.

Schaffer AE, Eggens VR, Caglayan AO, Reuter MS, Scott E, Coufal NG, Silhavy JL, Xue Y, Kayserili H, Yasuno K, et al (2014). CLP1 founder mutation links tRNA splicing and maturation to cerebellar development and neurodegeneration. *Cell* **157(3):**651-663.

Weitzer S, and Martinez J (2007). The human RNA kinase hClp1 is active on 3′ transfer RNA exons and short interfering RNAs. *Nature* **447**:222-226.

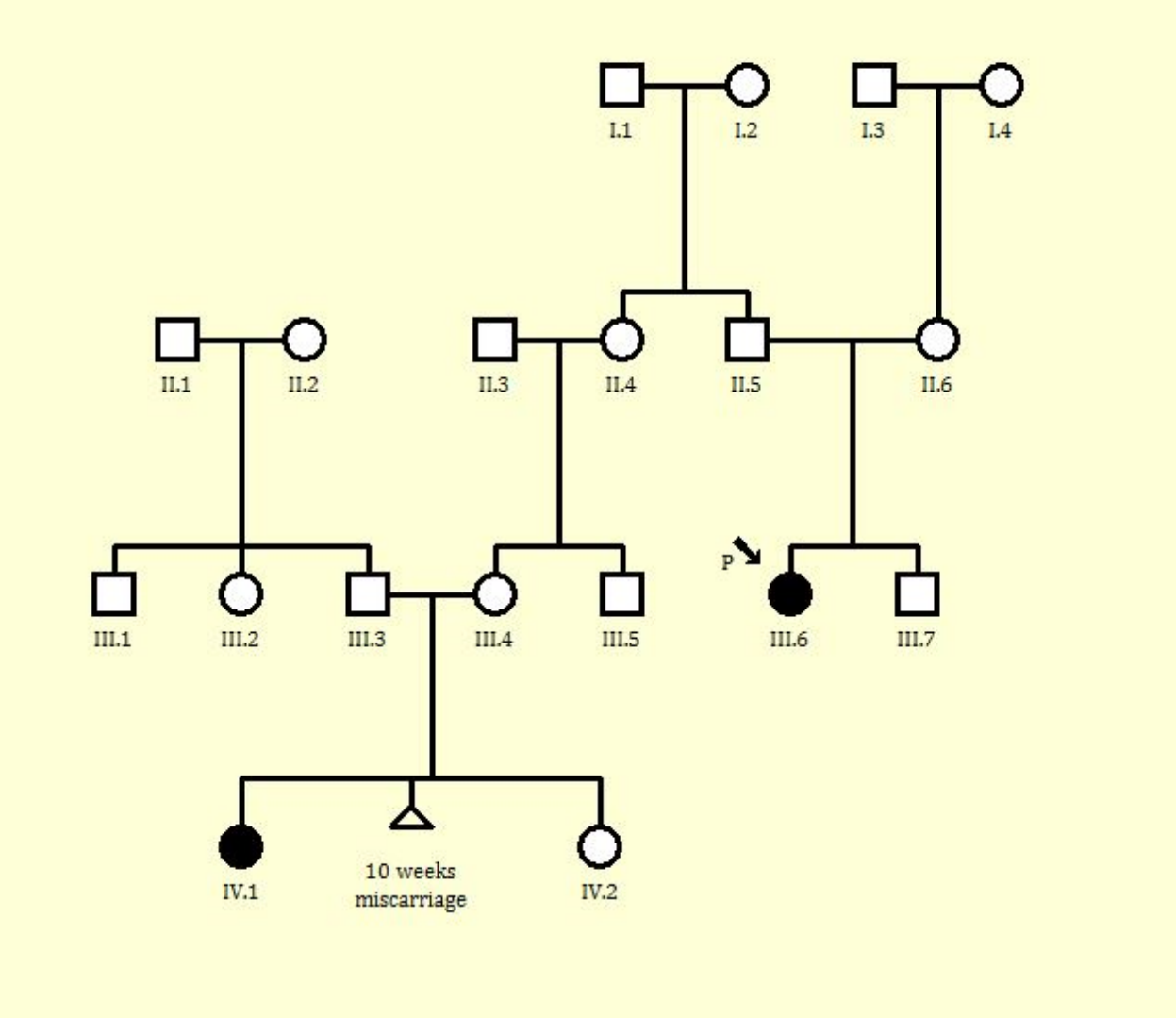

Fig.1 Pedigree showing the proband (III.6) and the proband's first cousin once removed (IV.1). Filled symbols represent affected individuals and open symbols represent unaffected individuals.

Fig.2(A)

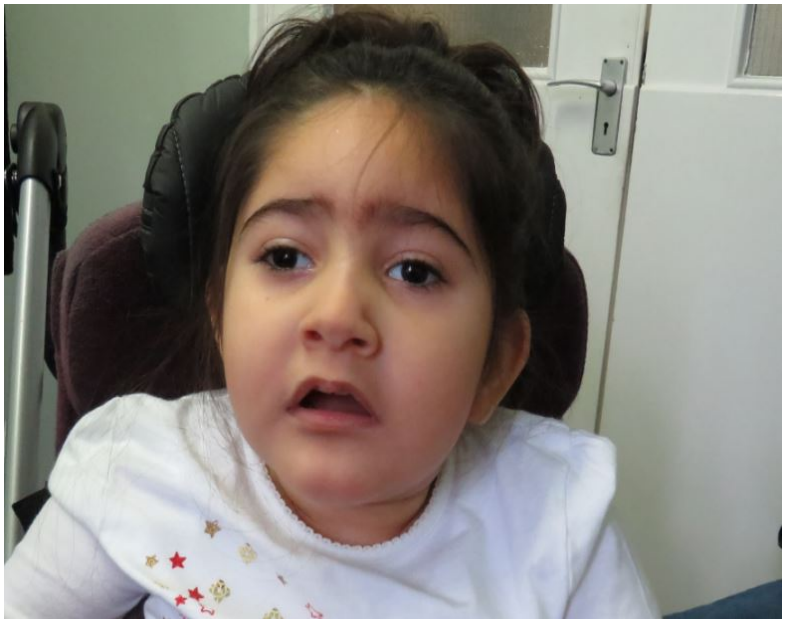

Fig.2(B)

Fig.3 Clinical photograph of IV.1 aged 5 years demonstrating more significant dysmorphic features in the form of marked synophrys, long palpebral fissures, divergent squint, broad nasal root, low hanging columella, widely spaced teeth, and a short neck.

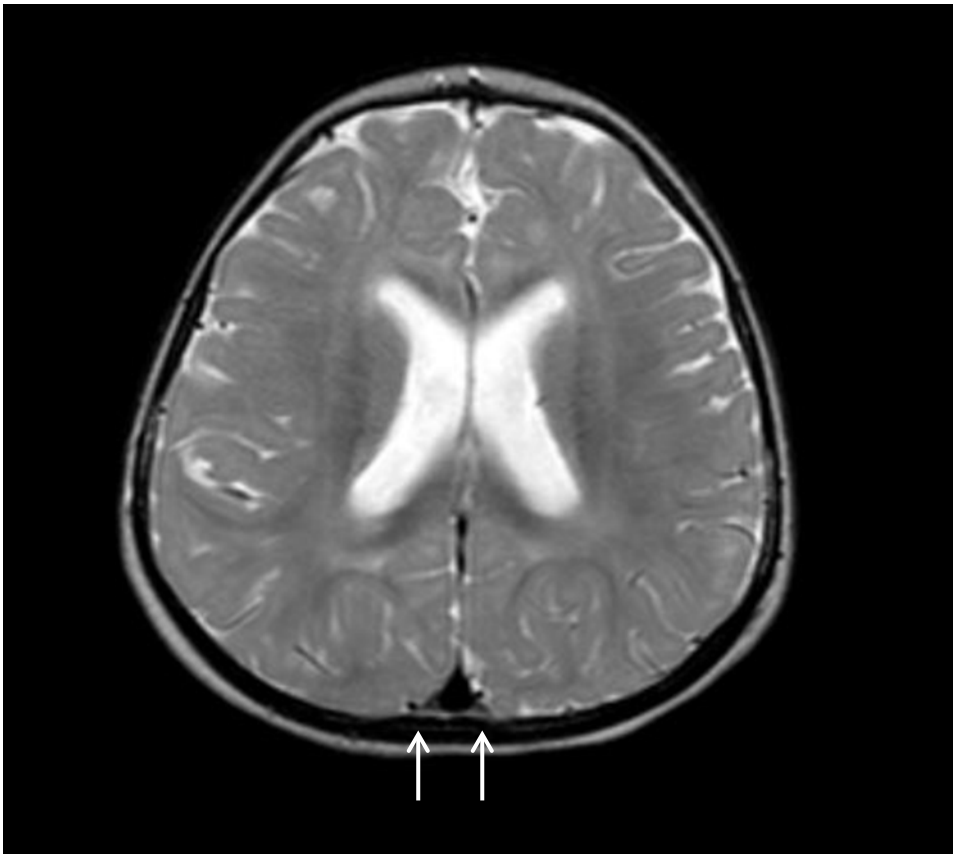

Fig.4(A) MRI brain scan of III.6 at 2 years. The axial transverse weighted image (A) shows thinning of the posterior aspect of both cerebral hemispheres, as indicated by the double white arrowheads.

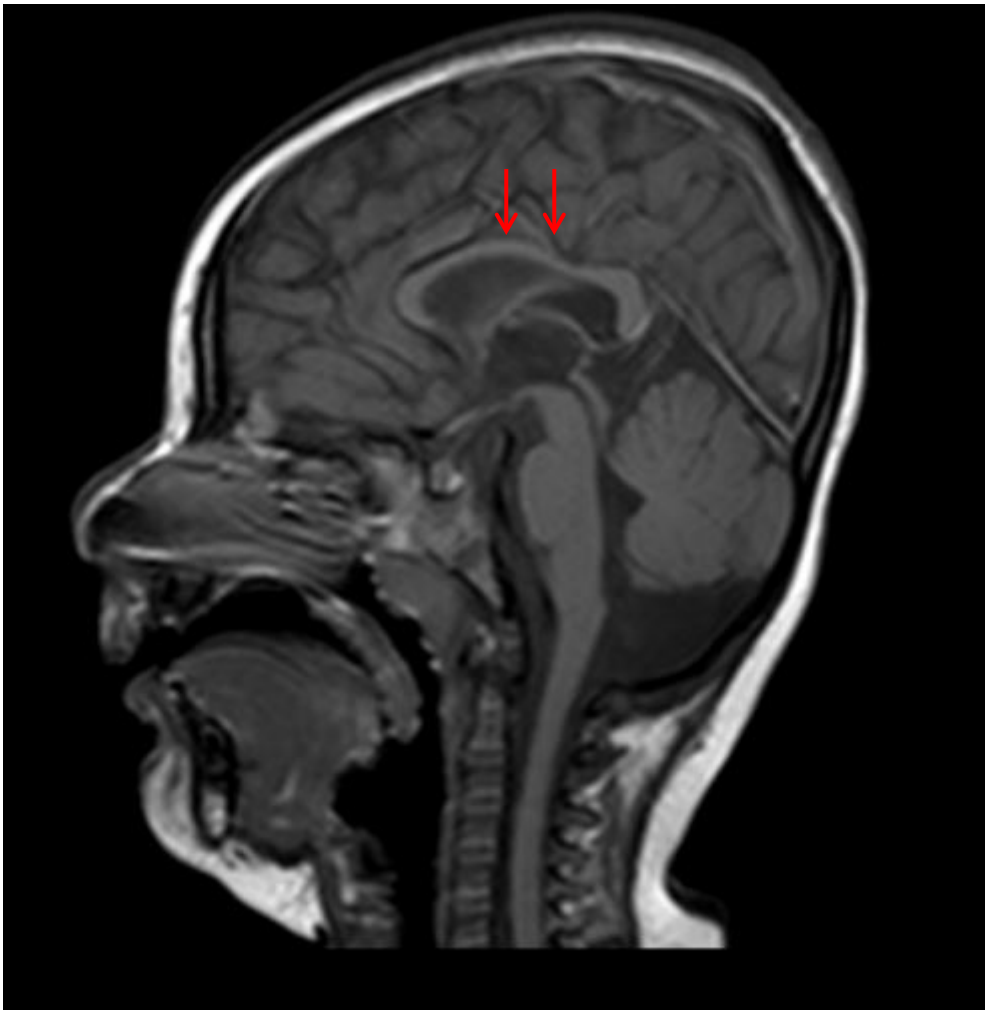

Fig.4(B) MRI brain scan of III.6 at 2 years. The sagittal weighted image (B) shows a reduction in the bulk of the corpus callosum as indicated by the red arrow heads.

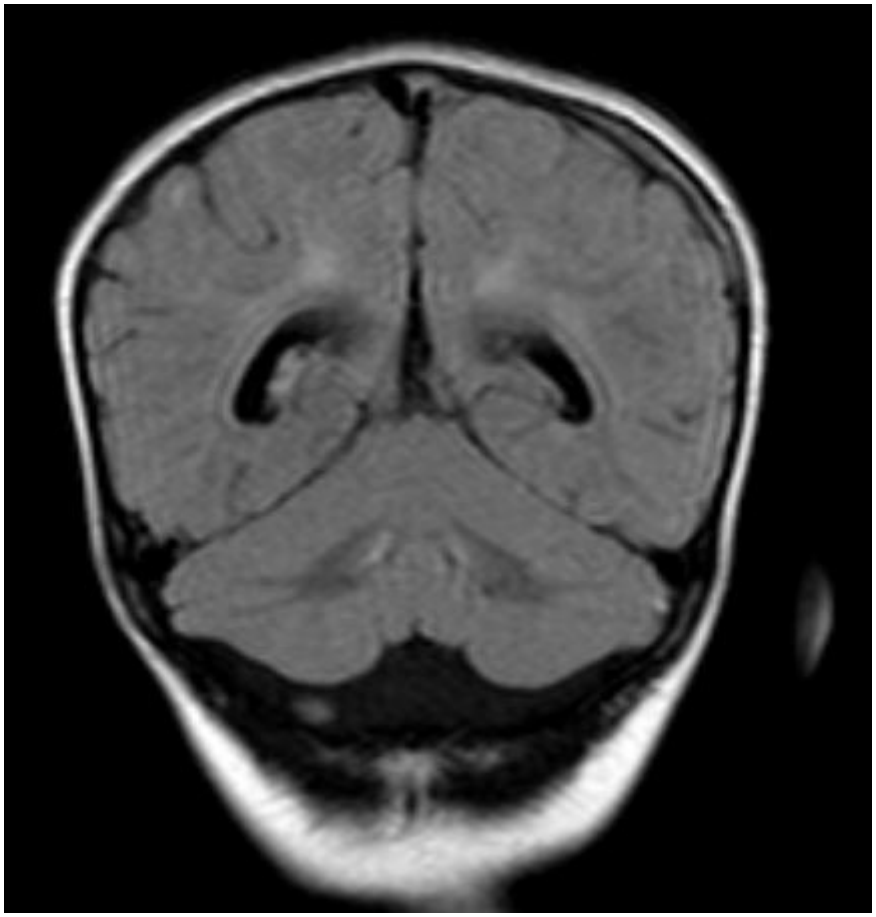

Fig.4(C) MRI brain scan of III.6 at 2 years. The coronal image (C) does not show evidence of cerebellar abnormalities.

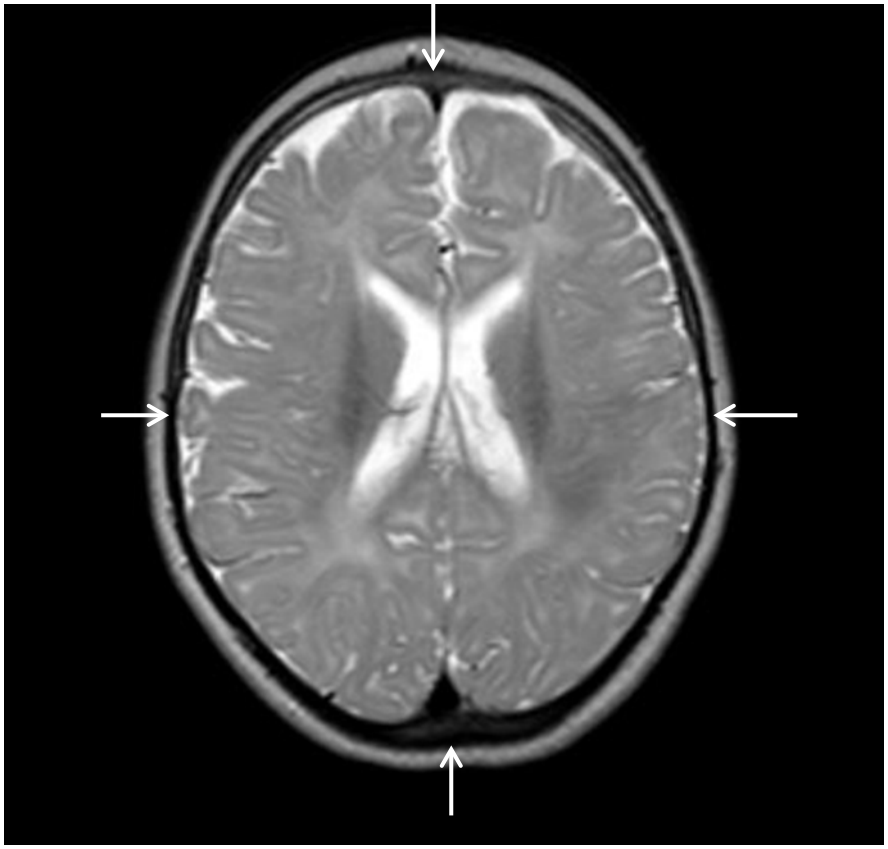

Fig.5(A) MRI brain scan of IV.1 at 3 years. The axial transverse weighted image (A) shows global reduction in white matter volume, as indicated by the white arrowheads, and a compensatory increase in extra-axial CSF space depth.

Fig.5(B) MRI brain scan of IV.1 at 3 years. The sagittal weighted image (B) shows mild loss of bulk within the pons and the midbrain as indicated by the double white arrowheads. There is a reduction in the bulk of the corpus callosum (indicated by double red arrowheads) as a consequence of generalized white matter volume loss.

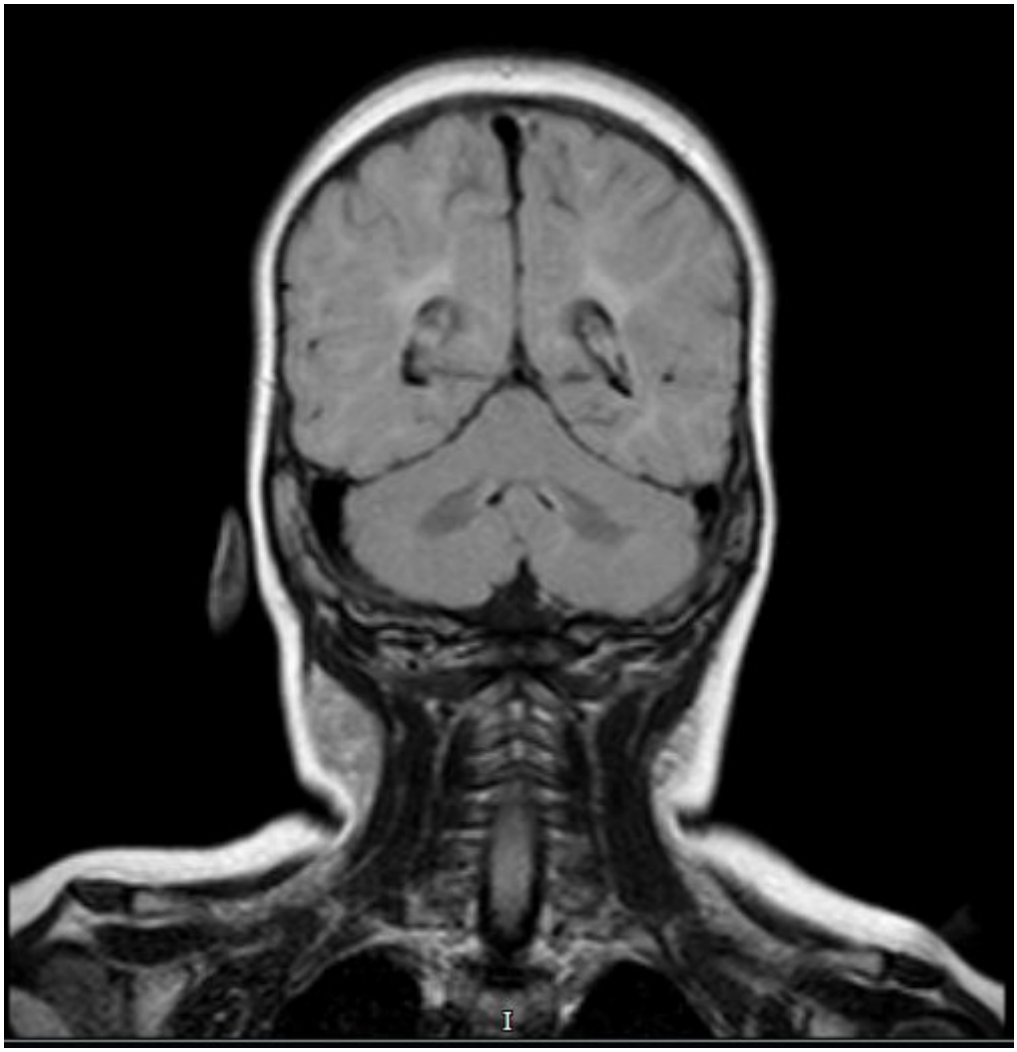

Fig.5(C) MRI brain scan of IV.1 at 3 years. The coronal image (C) does not show evidence of cerebellar abnormalities.

		III.6	IV.1
Dysmorphic features previously described in PCH10 (Karaca *et al*., and Schaffer *et al*., 2014)	High arched eyebrows	+	+
	Prominent eyes	–	–
	Long palpebral fissures	–	+
	Broad nasal root	+	+
	Alae nasi hypoplasia	+	+
Additional dysmorphic features	Bi-temporal narrowing	–	+
	Synophrys	–	+
	Bulbous nasal tip	–	+
	Low hanging columella	+	++
	Widely spaced teeth	–	+
	Short neck	–	+
	Tapered fingers	+	+
	Upper and lower limb hypertrichosis	+	++

Table 1. Summary of the dysmorphic features observed in III.6 and IV.1.

Test	III.6	IV.1
Plasma ammonia	Normal	Normal
Lactate	Normal	Normal
Plasma and urine amino acids	Normal	Normal
Urine organic acids	Normal	Normal
Karyotype	46, XX Normal	N/A
MECP2 and CDKL5 sequence and dosage analysis	Normal	N/A
Angelman syndrome (methylation and copy number analysis of 15q11-q13)	Normal	N/A
Microcephaly-capillary malformation syndrome (STAMBP sequencing)	No pathogenic mutation identified	N/A
Exome sequence analysis of targeted 91 gene panel associated with microcephaly and pontocerebellar hypoplasia	No pathogenic variant detected within the analysed regions	N/A
Array CGH	No significant abnormality detected	No significant abnormality detected

Table 2. List of metabolic and genetic investigations performed for III.6 and IV.1 prior to whole exome sequencing. N/A: not available.

		III.6	IV.1	Schaffer et al., 2014 (8 patients)
MRI findings	Cerebellum	No abnormality reported	No abnormality reported	Atrophy (6/6) 2 N/A
	Pons	No abnormality reported	Mild pontine hypoplasia	Hypoplasia (6/6) 2 N/A
	Cerebral cortex	Global white matter volume reduction affecting the posterior aspect of both cerebral hemispheres predominantly	Global white matter volume reduction	Atrophy (6/6) 2 N/A
	Ventricles	Large ventricles and prominent extra-axial CSF spaces	Large ventricles and prominent extra-axial CSF spaces	Enlarged (4/6) 2 N/A
	Corpus callosum	Thin	Thin	Thin (6/6) 2/NA
	Incidental findings	Prominent cysterna magna Syringomyelia	Prominent cysterna magna	NA

Table 3. List of MRI brain scan findings in III.6 and IV.1 compared to the previously reported 8 cases by Schaffer *et al*., 2014. N/A: not available.

		III.6	IV.1	Schaffer *et al*., 2014 (8 patients)
Growth parameters	Birth weight	3.5 kg	3.46 kg	Range (2.48-3.5 kg)
	Birth head circumference	34 cm (z-score: 0.10)	33.5 cm (z-score: −0.31)	Range (0/-2SD)
	Head circumference/examination age	41 cm/18 months (z-score: −3.79)	44.7 cm/ 3 years (z-score: −2.69)	Range (-1/-10 SD)
Development	Gross motor	Delayed/Absent	Delayed/Absent	Delayed/Absent(5/8) Delayed (3/8)
	Fine motor	Delayed	Delayed	Absent (5/8) Delayed (3/8)
	Language	Significant delay	Absent	Absent (5/8) Delayed (3/8)
	Cognitive	Delayed	Absent	Delayed (3/8) Delayed/Absent (3/8) Absent (2/8)
	Social	Delayed	Absent	Delayed (8/8)
Intellectual disability		+	++	8/8
Seizures	Seizures	+	_	6/8
	Seizure onset	3 years		Range (50 days-3 years)
Neurological findings	Hypotonia	+ (truncal hypotonia and head lag)	+ (truncal hypotonia and head lag)	3/8
	Hypertonia	+ (in all limbs)	+ (in upper limbs)	5/8

	Spasticity	_	++(in upper limbs)/++ contractures	5/8
	Deep tendon reflexes	Increased (in all limbs)	Increased (in all limbs)	Increased (6/8) Decreased (2/8)
	Jitteriness/clonus	+	_	1/8
Visual findings	Central visual impairment	_	+ (delayed visual maturation)	1/5 3 N/A
	Visual acuity	NR	6/38	N/A
	Cone-rod dystrophy	_	+ (with preservation of macular pathway function)	N/A
	Primary Optic atrophy	_	_	1/5 3 N/A
	Following and fixation	+	+/-	+ (2/5) +/- (2/5) - (1/5) 3 N/A
	Strabismus	+	+	1/5 3 N/A
	Nystagmus	_	+	1/5 3 N/A
	Hypermetropia	_	+	N/A
	Astigmatism	_	+	N/A
Skeletal abnormalities	Kyphoscoliosis	+	+	N/A
	Hip abnormalities	+ (developmental dysplasia of the hip)	+ (bilateral hip subluxation)	N/A
GIT manifestations	Constipation	++	+	N/A
	Feeding difficulties	+	+	N/A
	Gastro-oesophageal reflux disease	+	-	N/A
Vascular abnormalities		3 Cutaneous capillary malformations (right foot, right leg, and	_	N/A

	left buttock)		

Table 4. List of clinical features in III.6 and IV.1 compared to the previously reported 8 cases by Schaffer *et al*., 2014. N/A: not available.